Scrambling of quantum information in quantum many-body systems

Eiki Iyoda and Takahiro Sagawa
Department of Applied Physics, The University of Tokyo, 7-3-1 Hongo, Bunkyo-ku, Tokyo 113-8656, Japan

(Received 24 April 2017; revised manuscript received 10 February 2018; published 18 April 2018)

We systematically investigate scrambling (or delocalizing) processes of quantum information encoded in quantum many-body systems by using numerical exact diagonalization. As a measure of scrambling, we adopt the tripartite mutual information (TMI) that becomes negative when quantum information is delocalized. We clarify that scrambling is an independent property of the integrability of Hamiltonians; TMI can be negative or positive for both integrable and nonintegrable systems. This implies that scrambling is a separate concept from conventional quantum chaos characterized by nonintegrability. Specifically, we argue that there are a few exceptional initial states that do not exhibit scrambling, and show that such exceptional initial states have small effective dimensions. Furthermore, we calculate TMI in the Sachdev-Ye-Kitaev (SYK) model, a fermionic toy model of quantum gravity. We find that disorder does not make scrambling slower but makes it smoother in the SYK model, in contrast to many-body localization in spin chains.

DOI: 10.1103/PhysRevA.97.042330

I. INTRODUCTION

Whether or not an isolated system thermalizes is a fundamental issue in statistical mechanics, which is related to the nonintegrability of Hamiltonians. In classical systems, thermalization has been discussed in terms of the ergodicity of chaotic systems [1]. In quantum systems, a counterpart of classical chaos is not immediately obvious because the Schrödinger equation is linear. Nevertheless, it has been established that there are some indicators of chaotic behaviors in quantum systems, such as the level statistics of Hamiltonians [2–4] and decay of the Loschmidt echo [5,6]. More recently, the eigenstate-thermalization hypothesis (ETH) [7–11] has attracted attention as another indicator of quantum chaos in many-body systems, which states that even a single-energy eigenstate is thermal. All these indicators of quantum chaos are directly related to the integrability of Hamiltonians; nonintegrable quantum systems exhibit chaos. Such a chaotic behavior in isolated quantum systems is also a topic of active research in real experiments with ultracold atoms [12–14], trapped ions [15], NMR [5], and superconducting qubits [16].

In order to investigate the "chaotic" properties of quantum many-body systems beyond the conventional concept of quantum chaos, it is significant to focus on the dynamics of quantum information encoded in quantum many-body systems. How does locally encoded quantum information spread out over the entire system by unitary dynamics? Such delocalization of quantum information is referred to as *scrambling* [17–21]. Investigating scrambling is important not only for understanding the relaxation dynamics of experimental systems at hand, but also in terms of the information paradox of black holes [17], where it has been argued that black holes are the fastest scramblers in the universe [18]. However, the fundamental relationship between scrambling and conventional quantum chaos has not been comprehensively understood.

Scrambling can be quantified by the tripartite mutual information (TMI) [21,22], which becomes negative if quantum information is scrambled. There is also another measure of scrambling, named the out-of-time-ordered correlator (OTOC) [20,21,23–30]. It has been argued that the decay rate of the OTOC is connected to the Lyapunov exponent in the semiclassical limit [23]. TMI and OTOC capture essentially the same feature of scrambling [21], where OTOC depends on a choice of observables but TMI does not. In the context of the holographic theory of quantum gravity, TMI is shown negative [31] if the Ryu-Takayanagi formula [32] is applied, suggesting that gravity has a scrambling property. This is consistent with fast scrambling in the Sachdev-Ye-Kitaev (SYK) model [23,33–40], a toy model of a quantum black hole. Then, a natural question raised is to what extent such a property of quantum gravity is intrinsic to gravity or can be valid for general quantum many-body systems.

In this paper, we perform systematic numerical calculations of real-time dynamics of TMI in quantum many-body systems under unitary dynamics, by using exact diagonalization of Hamiltonians. We consider a small system (say, a qubit) and a quantum many-body system (say, a spin chain). The information of the small system is initially encoded in the many-body system through entanglement. The many-body system then evolves unitarily, and we observe how the locally encoded information is scrambled over the entire many-body system. We note that temporal TMI has been investigated by using the channel-state duality in Ref. [21], while here we calculate instantaneous TMI, with which we can study the role of the initial states.

By studying quantum spin chains such as the *XXX* model and the transverse-field Ising (TFI) model with and without integrability breaking terms, we find that scrambling occurs (i.e., TMI becomes negative) for both the integrable and nonintegrable systems for a majority of the initial states. On the other hand, for a few exceptional initial states, scrambling does not occur (i.e., TMI becomes positive) for both the integrable and nonintegrable cases of the *XXX* model. We also show that these exceptional states have small effective dimensions.

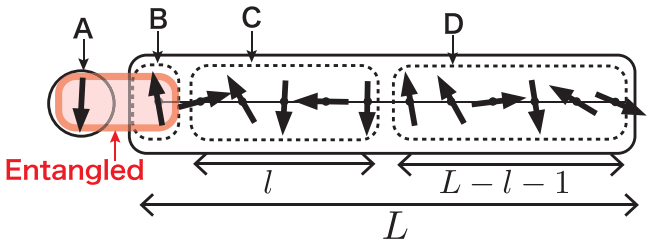

FIG. 1. Schematics of our setup. Initially, qubit A is maximally entangled with qubit B, while C and D are not correlated with A and B. Then, BCD evolves unitarily with a Hamiltonian that is either integrable or nonintegrable, and either clean or disordered. We calculate the real-time dynamics of TMI between A, B, and C.

These results clarify that scrambling is an independent property of the integrability of Hamiltonians. Therefore, scrambling does not straightforwardly correspond to conventional quantum chaos, making a sharp contrast to the level statistics and ETH. We remark that the relationship between integrability and ballistic entanglement spreading has been studied [41–43], while delocalization and entanglement spreading capture different aspects of information dynamics [44], as will be discussed later in detail.

We also consider the SYK model with four-body interaction of complex fermions, and find that disorder does not lead to slow dynamics but instead makes scrambling smoother than a clean case. This is in contrast to the slow scrambling in the many-body localized (MBL) phase of a spin chain [45–52].

The rest of this paper is organized as follows. In Sec. II, we formulate our setup and introduce TMI. In Sec. III, we show our main numerical results. We first discuss the relationship between scrambling and integrability with one-dimensional quantum spin systems. We also investigate the effect of disorder in the MBL phase and the SYK model. In Sec. IV, we summarize our results. In the Appendix, we show some supplemental numerical results.

II. SETUP

A. System and initial state

We consider either a spin-1/2 or a fermionic system on a lattice, which consists of small system A on a single site and a many-body system on L sites (Fig. 1). The many-body system is divided into three subsystems B, C, and D, whose sizes (the numbers of the lattice sites) are, respectively, given by $1, l$, and $L-l-1$. The lattice structure BCD is supposed to be one dimensional for spin chains or all connected for the SYK model. For a single site of a spin (fermion) system, we write $|0\rangle$ as the spin-up (particle-occupied) state, and $|1\rangle$ as the spin-down (particle-empty) state. In any case, a single qubit is on a single site.

We first prepare a product state,

$$\frac{1}{\sqrt{2}}(|0\rangle_{\mathrm{A}}+|1\rangle_{\mathrm{A}})\otimes|\Xi\rangle_{\mathrm{BCD}}, \tag{1}$$

where $|\Xi\rangle_{\mathrm{BCD}}$ is a product state with the state of each qubit being $|0\rangle$ or $|1\rangle$ (e.g., the Néel state $|0\rangle|1\rangle|0\rangle\cdots|0\rangle|1\rangle$ or the all-up state $|0\rangle|0\rangle\cdots|0\rangle$, etc.). We then apply the CNOT gate on the state (1), where the control qubit is A and the target qubit is B. By this CNOT gate, information about A is locally encoded in B through entanglement. Then, only BCD obeys a unitary time evolution with a time-independent Hamiltonian. We calculate the time dependence of TMI between A, B, and C, which characterizes scrambling of the information about A that was initially encoded in B. We note that the foregoing setup is associated with a thought experiment that one of the qubits of an Einstein-Podolsky-Rosen (EPR) pair is thrown into a black hole and then scrambled [17].

B. Tripartite mutual information

We next consider TMI. Let X, Y, and Z be subregions of the lattice (i.e., subsets of the lattice sites). The bipartite mutual information (BMI) is defined as $I_2(X:Y):=S_{\mathrm{X}}+S_{\mathrm{Y}}-S_{\mathrm{XY}}$, where $S_{\mathrm{X}}:=\mathrm{tr}_{\mathrm{X}}[-\hat{\rho}_{\mathrm{X}}\ln\hat{\rho}_{\mathrm{X}}]$ is the von Neumann entropy of a reduced density operator $\hat{\rho}_{\mathrm{X}}:=\mathrm{tr}_{\mathrm{X}^{\mathrm{c}}}[\hat{\rho}]$, with X^{c} being the complemental set of X. Then, TMI is defined by [21,22]

$$I_3(X:Y:Z):=I_2(X:Y)+I_2(X:Z)-I_2(X:YZ). \tag{2}$$

Here, TMI is negative when $I_2(X:Y)+I_2(X:Z)<I_2(X:YZ)$, which implies that information about X stored in composite YZ is larger than the sum of the amounts of information that Y and Z have individually; information about X is delocalized to Y and Z in such a case.

To illustrate the meaning of TMI, let us consider three classical bits x,y,z and the following situations: (i) $I_3(x:y:z)=-\ln 2$, if $x=y\oplus z$ and y,z are independent and random, where $\oplus$ describes the binary sum. In this case, neither y nor z is individually correlated with x, but composite yz is maximally correlated with x. (ii) $I_3(x:y:z)=0$, if x,y, and z are all independent and random. In this case, there is no correlation between x,y, and z. (iii) $I_3(x:y:z)=\ln 2$, if $x=y=z$ and x is random. In this case, the three bits form the maximum three-body correlation.

While the above examples are classical, a similar argument applies to quantum situations. In fact, TMI can be utilized to characterize nonlocal and long-range entanglement in topological orders [53].

III. NUMERICAL RESULTS

In this section, we show our main results on one-dimensional spin chains and the SYK model.

A. Scrambling and integrability

We first discuss scrambling in the XXX model in one dimension with and without an integrability breaking term. The Hamiltonian is given by

$$\hat{H}_{\mathrm{XXX}}:=\sum_{\langle i,j\rangle}J\boldsymbol{\sigma}_i\cdot\boldsymbol{\sigma}_j+\sum_{\langle\langle i,j\rangle\rangle}J'\boldsymbol{\sigma}_i\cdot\boldsymbol{\sigma}_j, \tag{3}$$

where i and j are indices of sites, and $\langle i,j\rangle$ and $\langle\langle i,j\rangle\rangle$ mean that i and j run within nearest neighbor (NN) and next-nearest neighbor (NNN), respectively. The Pauli matrices for a spin are written as σ_i^{α} $(\alpha=x,y,z)$, and we define $\boldsymbol{\sigma}_i:=(\sigma_i^x,\sigma_i^y,\sigma_i^z)$. Let $J>0$. This model is integrable if $J'=0$, while it is nonintegrable if $J'>0$.

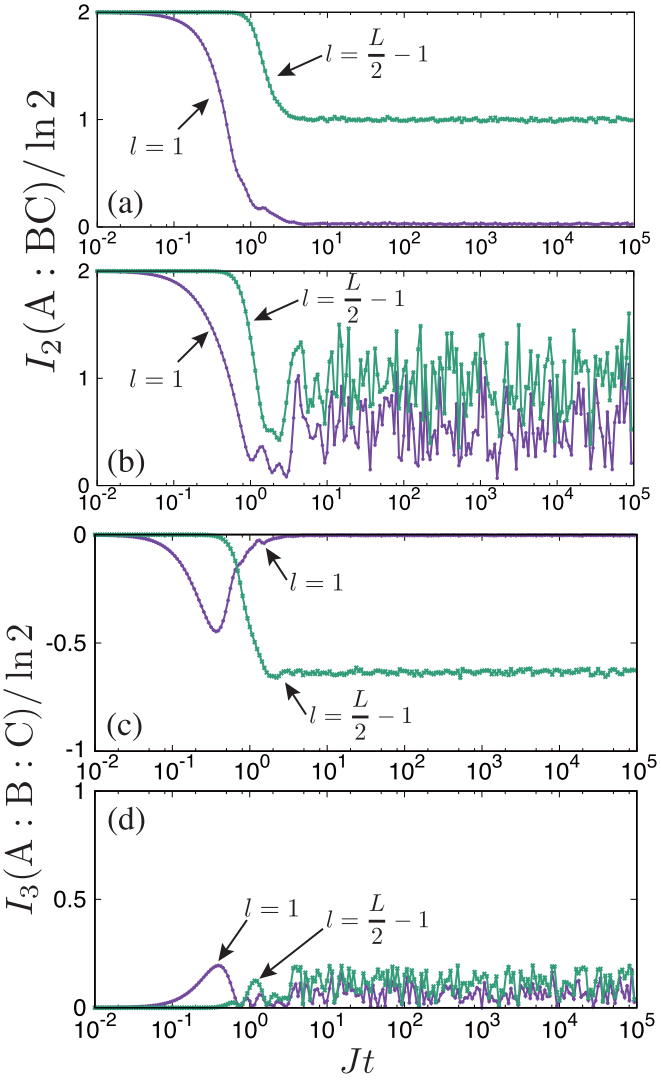

FIG. 2. Time dependence of BMI and TMI for the nonintegrable *XXX* model with parameters $L = 14, J' = 0.8J$, and $l = 1$ or $L/2 - 1$. The information content and the initial state are (a) BMI, Néel, (b) BMI, all up, (c) TMI, Néel, and (d) TMI, all up.

We consider the nonintegrable case with $J' = 0.8J$ in Eq. (3), where the parameters are taken so that the level statistics is the Wigner-Dyson distribution [4], implying that the system is fully chaotic in the sense of conventional quantum chaos. Figures 2(a) and 2(b) show the time dependence of BMI $I_2(A : BC)$ with the initial state being (a) Néel or (b) all up, along with TMI $I_3(A : B : C)$ in Figs. 2(c) and 2(d).

At initial time $t = 0$, BMI is given by $2 \ln 2$ because of the entanglement between A and B. As time increases, BMI decays for all the cases. In Fig. 2(a), the decay is much smoother, where BMI saturates at zero for $l = 1$ and at $\ln 2$ for $l = L/2 - 1$. These are consistent with the behaviors of TMI as discussed below.

Figure 2(c) shows that TMI becomes negative for the initial Néel state, implying scrambling. For $l = 1$, TMI decreases from zero, goes through a minima, and gradually returns to zero. This means that information is scrambled inside ABC in a short-time regime, and then completely disappears from BC in a longer-time regime. For $l = L/2 - 1$, TMI monotonically decreases and saturates at a negative value. This means that information is scrambled but is not totally lost from BC, even in a long-time regime. These results are consistent with the behaviors of BMI.

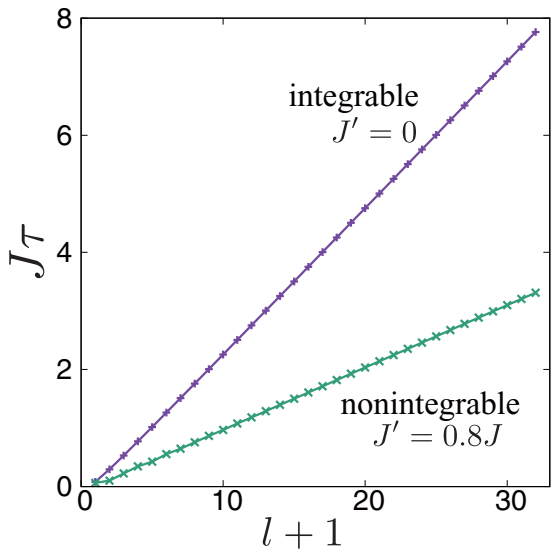

FIG. 3. Dependence on the subsystem size of the decay time τ of BMI. The system size is $L = 128$ and the initial state is all up.

On the other hand, as shown in Fig. 2(d), TMI is positive when the initial state is all up. In this case, information is not scrambled, but a three-body correlation forms among A, B, and C. We remark that entanglement spreads ballistically even in this case. Figure 3 shows the decay time τ, at which $I_2(A : BC)$ becomes $a \ln 2$ $(0 < a < 2)$ for the first time. The constant a can be arbitrarily chosen and here we set $a = 1.9$. Figure 3 clearly shows the linear dependence of τ on l, which implies that entanglement spreads ballistically. This clarifies that what TMI characterizes is delocalization of quantum information, rather than ballistic spreading of entanglement. More detailed results on entanglement spreading are shown in the Appendix.

We next discuss the integrable case with $J' = 0$ in Eq. (3). Figure 4 shows the time dependence of TMI for the initial state being (a) Néel or (b) all up. The qualitative behavior of TMI is similar to the nonintegrable case; scrambling occurs in Fig. 4(a) but does not in Fig. 4(b). We do not observe recurrence induced by integrability because our system size is sufficiently large.

We therefore conclude that scrambling occurs independently of integrability. We note that the time range of our numerical simulation is sufficiently long to see the role of nonintegrability. In fact, the level spacing at the peak of the Wigner-Dyson distribution corresponds to $Jt \simeq 10^3$ in our nonintegrable model [55]. We also note that our numerical simulation is not restricted to the low-energy states, which can be effectively described by the integrable field theory [56].

To study the initial-state dependence of scrambling more systematically, we calculated the *XXX* model with all possible product states, $|\Xi\rangle_{\mathrm{BCD}}$. We label 2^L product states in the computational basis by bit sequences from $|000\cdots0\rangle$ to $|111\cdots1\rangle$. Figure 5 shows the initial-state dependence of the maximum and minimum values of TMI in $0 \leqslant Jt < 10^5$,

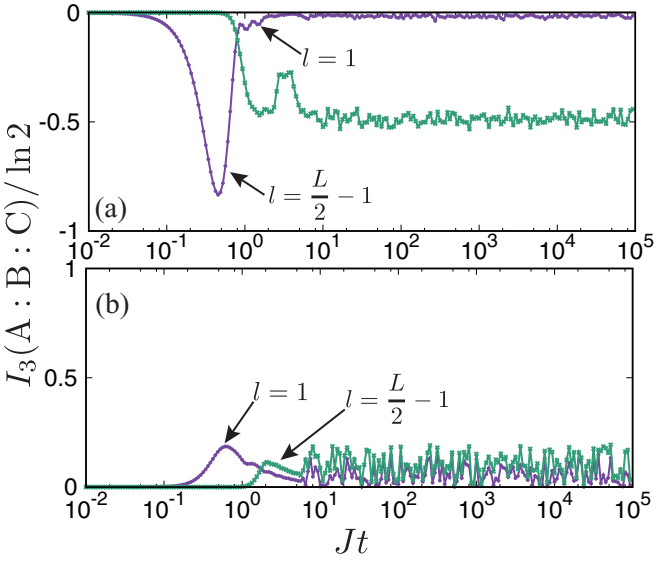

FIG. 4. Time dependence of TMI for the integrable *XXX* model with parameters $L = 14, J' = 0$, and $l = 1$ or $L/2 - 1$. The initial state is (a) Néel and (b) all up.

written as $I_3^{\max}$ and $I_3^{\min}$, respectively, for (a) nonintegrable and (b) integrable cases. The horizontal axis shows the labels of $|\Xi\rangle_{\mathrm{BCD}}$ in decimal. We see that scrambling occurs ($I_3^{\min} < 0$) for most of the initial states.

On the other hand, there are only four initial states with which scrambling does not occur ($I_3^{\min} = 0$) for both Fig. 5(a) and Fig. 5(b). These four states are $|0\rangle|0\rangle|0\rangle\cdots|0\rangle$, $|1\rangle|0\rangle|0\rangle\cdots|0\rangle$, $|0\rangle|1\rangle|1\rangle\cdots|1\rangle$, and $|1\rangle|1\rangle|1\rangle\cdots|1\rangle$. The reason why these four states are exceptional is that the Hamiltonian (3) conserves the total magnetization in the z direction. This confines the dynamics into a much smaller subspace of the Hilbert space, which leads to the absence of scrambling.

In order to clarify the relationship between the initial state and scrambling, we consider the effective dimension of the

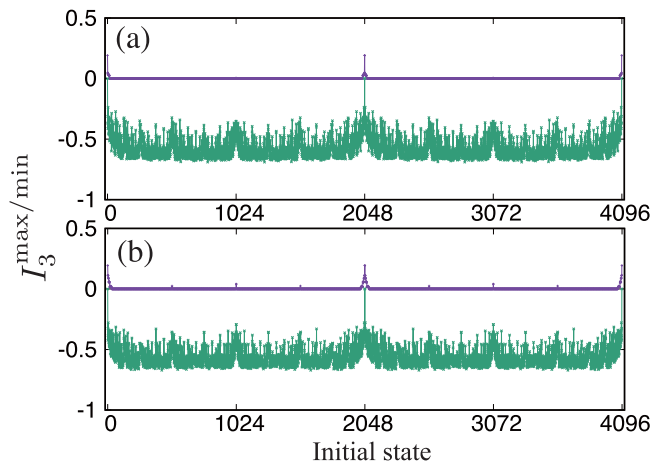

FIG. 5. Initial-state dependence of the maximum (purple) and the minimum (green) values of TMI for the *XXX* model with parameters $L = 12, l = L/2 - 1$. (a) Nonintegrable case ($J' = 0.8J$), (b) integrable case ($J' = 0$).

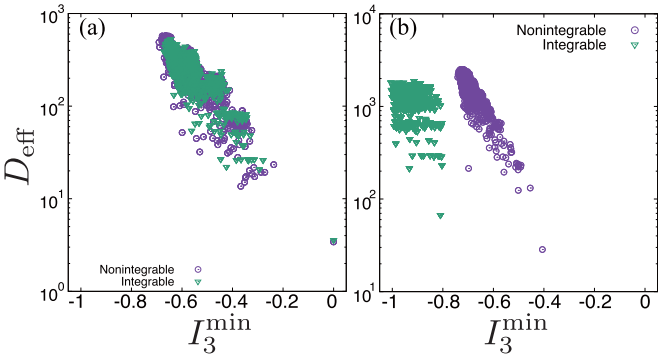

FIG. 6. Effective dimension D_{eff} vs the minimum value of TMI, $I_3^{\min}$. Parameters are $L = 12$ and $l = L/2 - 1$. (a) *XXX* model, (b) TFI model.

initial state, which is known to characterize the relaxation process in isolated quantum systems. In particular, a large effective dimension leads to relaxation of the expectation value of an observable in the long-time regime [54]. Let the initial state be $|\Psi\rangle = \sum_i \sum_{\alpha=1}^{d_i} c_{i,\alpha}|E_{i,\alpha}\rangle$, where $|E_{i,\alpha}\rangle$ is the eigenstate of the Hamiltonian with the eigenenergy $E_{i,\alpha}$. Here, $E_{i,\alpha}$ (=:E_i) is independent of α, and d_i represents the degree of the degeneracy of E_i. The effective dimension of $|\Psi\rangle$ is defined as

$$D_{\mathrm{eff}} := \left(\sum_i p_i^2\right)^{-1}, \tag{4}$$

where $p_i := \sum_{\alpha=1}^{d_i} |c_{i,\alpha}|^2$ is the weight of E_i. We have calculated D_{eff} of all the separable states used in Fig. 5. Figure 6(a) shows a correlation between $I_3^{\min}$ and D_{eff}, i.e., $I_3^{\min}$ tends to be smaller when D_{eff} is larger. In particular, the above four exceptional states have very small effective dimensions, which is consistent with the conservation of the total magnetization in the z direction. Thus, this result suggests that if an initial state does not exhibit scrambling, it has a small effective dimension.

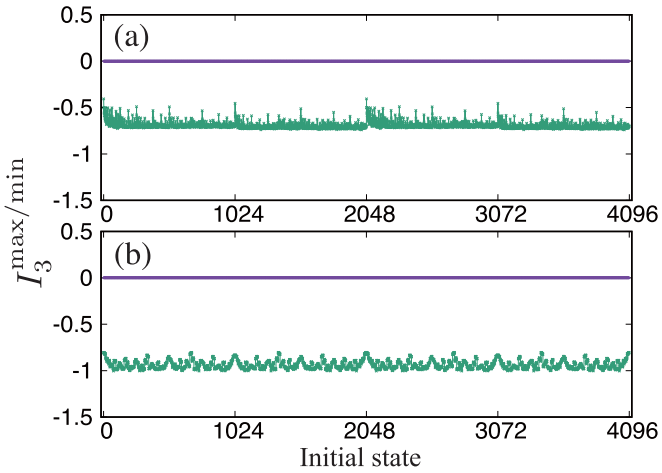

FIG. 7. Initial-state dependence of the maximum (purple) and the minimum (green) values of TMI for the TFI model with parameters $L = 12$ and $l = L/2 - 1$. (a) Nonintegrable case ($h_x = 2.1J$ and $h_z = 1.1J$), (b) integrable case ($h_x = J$ and $h_z = 0$).

We next consider TMI for the TFI model with and without an integrability breaking term. The Hamiltonian is given by

$$\hat{H}_{\rm TFI} := \sum_{\langle i,j\rangle} J\sigma_i^z\sigma_j^z + \sum_i h_x\sigma_i^x + \sum_i h_z\sigma_i^z. \qquad (5)$$

The transverse and longitudinal magnetic fields are given by $h_x = J$ and $h_z = 0$ for the integrable case, and by $h_x = 2.1J$ and $h_z = 1.1J$ for the nonintegrable case. Figure 7 shows that scrambling occurs for both the integrable and nonintegrable cases and for all of the initial product states in the computational basis.

The reason why scrambling occurs for the initial all-up state is that the total magnetization in the z direction is no longer conserved in the TFI model, and therefore quantum information is mixed up in a huge subspace. To support this observation, we have also calculated the effective dimension of the TFI model. Figure 6(b) shows a similar trend as is the case for the *XXX* model, while $D_{\rm eff}$ is overall larger than the case of the *XXX* model.

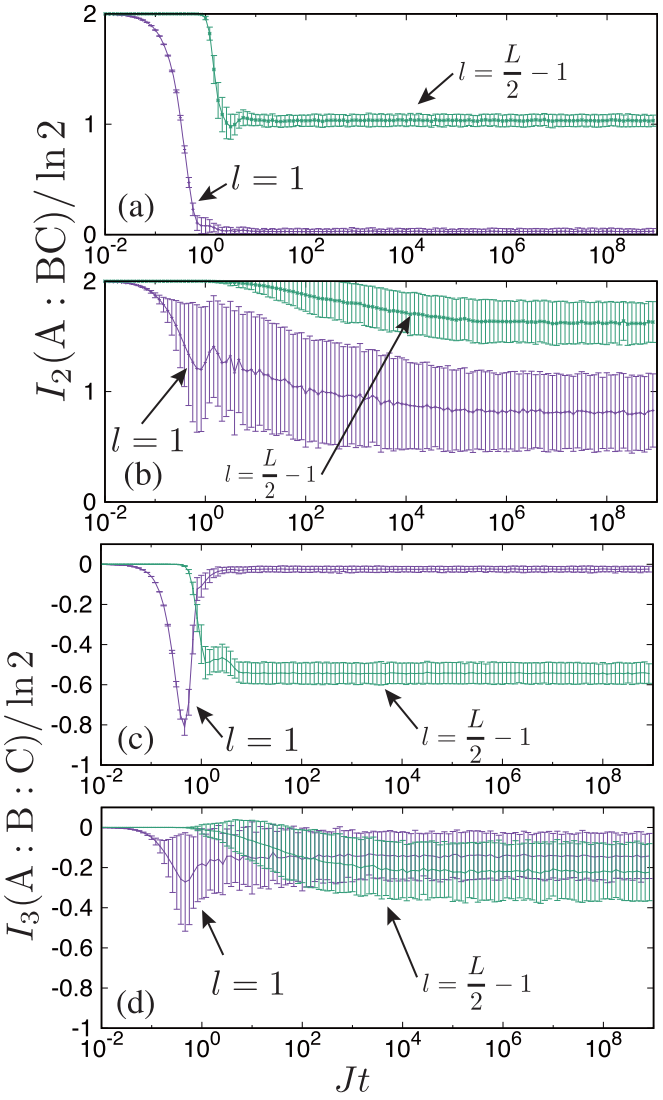

FIG. 8. Time dependence of BMI and TMI for the disordered *XXX* model with the initial Néel state with $L = 12$. The number of samples is 128. The information content and the phase are (a) BMI, ergodic ($h = J$), (b) BMI, MBL ($h = 10J$), (c) TMI, ergodic ($h = J$), and (d) TMI, MBL ($h = 10J$).

B. Many-body localized phase

We now consider the role of disorder by focusing on the disordered *XXX* model. The Hamiltonian is given by

$$\hat{H}_{\rm MBL} := \sum_{\langle i,j\rangle} J\boldsymbol{\sigma}_i\cdot\boldsymbol{\sigma}_j + \sum_i h_i\sigma_i^z, \qquad (6)$$

where h_i is a random magnetic field and is generated uniformly from $[-h,h]$ ($h > 0$). The amplitude of disorder h is $h = J$ for the ergodic phase and $h = 10J$ for the MBL phase.

Figure 8 shows the time dependence of BMI and TMI with the initial Néel state, where the ensemble average is taken over 128 samples and the error bars represent the standard deviations over the samples. In the ergodic phase, Figs. 8(a) and 8(c) are qualitatively the same as the clean cases [Figs. 2(a) and 2(c), and Figs. 4(a) and 4(c)]. In the MBL phase, Fig. 8(b) shows that BMI decays quite slowly. This is consistent with a phenomenology of local integrals of motion of MBL [47]. Figure 8(d) shows that the time scale of scrambling is similar to the clean case for $l = 1$, but is quite longer for $l = L/2 - 1$. This is also consistent with the phenomenology of MBL [47]. In fact, information can rapidly be scrambled in *ABC* if C is small, while scrambling should be quite slow if C is large because of the exponentially decaying interaction. In addition, Fig. 9 shows TMI with the initial all-up state, where scrambling does not occur in both the ergodic and the MBL phases.

C. Sachdev-Ye-Kitaev model

We next consider the SYK model [23,33–40] with complex fermions,

$$\hat{H}_{\rm SYK} := \frac{1}{(2L)^{3/2}} \sum_{i,j,k,l} J_{ij;kl} c_i^\dagger c_j^\dagger c_k c_l, \qquad (7)$$

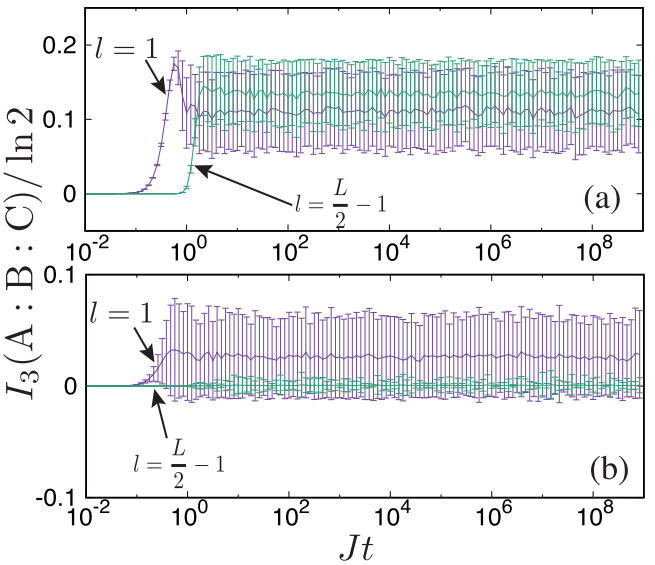

FIG. 9. Time dependence of TMI for the disordered *XXX* model with the initial all-up state with $L = 12$. The number of samples is 128. The phase are (a) ergodic ($h = J$) and (b) MBL ($h = 10J$).

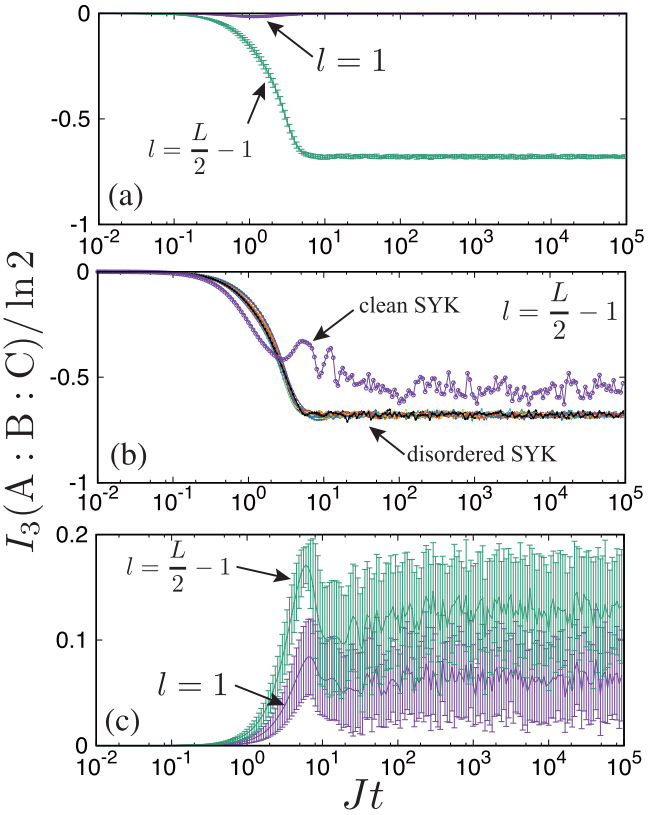

FIG. 10. Time dependence of TMI for the SYK model with parameters $L = 14$, and $l = 1$ or $L/2 - 1$. (a) Disordered SYK model with the initial Néel state. (b) Clean SYK model and typical samples of the disordered SYK model with the initial Néel state. (c) Disordered SYK model with the initial all-up state.

where $c_i^\dagger(c_i)$ is the creation (annihilation) operator of a fermion at site i. The coupling in the SYK model is all to all and four body (four local), and random: $J_{ij;kl}$ is sampled from the complex Gaussian distribution with variance J^2, satisfying $J_{ij;kl} = -J_{ji;kl} = -J_{ij;lk} = J^*_{lk;ji}$. We also consider a clean SYK model without disorder (i.e., $J_{ij;kl} \equiv J$ for $i > j, k > l$) in order to clarify the role of disorder.

Figure 10(a) shows the time dependence of TMI for the SYK model with the random coupling, where the initial state is Néel (i.e., fermions are half filled), the ensemble average is taken over 16 samples, and the error bars represent the standard deviations over the samples. In particular, TMI for $l = L/2 - 1$ monotonically decreases to a negative steady value. This smooth decrease is contrasted to the case of the clean SYK model shown in Fig. 10(b), where scrambling occurs but TMI exhibits large temporal fluctuations. We note that for typical disordered cases that are also shown in Fig. 10(b), scrambling is smoother even without taking the ensemble average. Therefore, disorder enhances scrambling in the case of the fermionic SYK model, as opposed to the case of MBL of spin chains.

In addition, Fig. 10(c) shows the case of the initial all-up state (i.e., $|0\rangle \cdots |0\rangle$), where TMI is positive and scrambling does not occur for both the disordered and clean cases. This is a consequence of the conservation of the fermion number, as is the case for the *XXX* model with the conservation of the initial magnetization.

TABLE I. Summary of our numerical results.

	Scrambled ($I_3 < 0$)	Not scrambled ($I_3 > 0$)
Nonintegrable	$XXX + J'$ (Néel)	$XXX + J'$ (all up)
	TFI + h_z (Néel, all up)	
Integrable	*XXX* (Néel)	*XXX* (all up)
	TFI (Néel, all up)	
	Clean SYK (Néel)	Clean SYK (all up)
Disordered	MBL (Néel)	MBL (all up)
	Disordered SYK (Néel)	Disordered SYK (all up)

IV. CONCLUDING REMARKS

We have systematically investigated the scrambling dynamics of quantum information in isolated quantum many-body systems, where we have adopted TMI as a measure of scrambling. We summarize the foregoing numerical results in Table I (see also the Appendix for supplemental results). We have observed that scrambling occurs independently of integrability, where an overwhelming majority of initial states exhibits scrambling for both the integrable and nonintegrable cases. We have also calculated the effective dimension to clarify the relationship between the initial state and scrambling, which shows that the exceptional initial states without scrambling have small effective dimensions. Although the connection between TMI and scrambling has already been established in previous works [21,22], our work has revealed that scrambling is a separate concept from conventional quantum chaos.

We have also investigated the MBL phase of a spin chain and the SYK model. We found that disorder makes scrambling smoother in the SYK model, which is contrastive to the case of the MBL spin chain. We postpone a more detailed analysis of the origin of this feature of the SYK model [57]. Here we only note that the clean SYK model is integrable, as shown in Table I [57].

We remark that experimental realizations of the SYK model have been theoretically proposed with ultracold atoms [38] and a solid-state device [58]. Furthermore, OTOC has experimentally been measured with trapped ions [59]. By using such state-of-the-art quantum technologies, the scrambling dynamics of quantum many-body systems can be investigated, and our results can be experimentally tested, which is a future issue.

ACKNOWLEDGMENTS

T.S. is grateful to M. Rigol for a valuable discussion. E.I. and T.S. are supported by JSPS KAKENHI Grant No. JP16H02211. E.I. is also supported by JSPS KAKENHI Grant No. JP15K20944. T.S. is also supported by JSPS KAKENHI Grant No. JP25103003.

APPENDIX: SUPPLEMENTAL NUMERICAL RESULTS

In this Appendix, we show some supplemental numerical results, which support the conclusions in the main text.

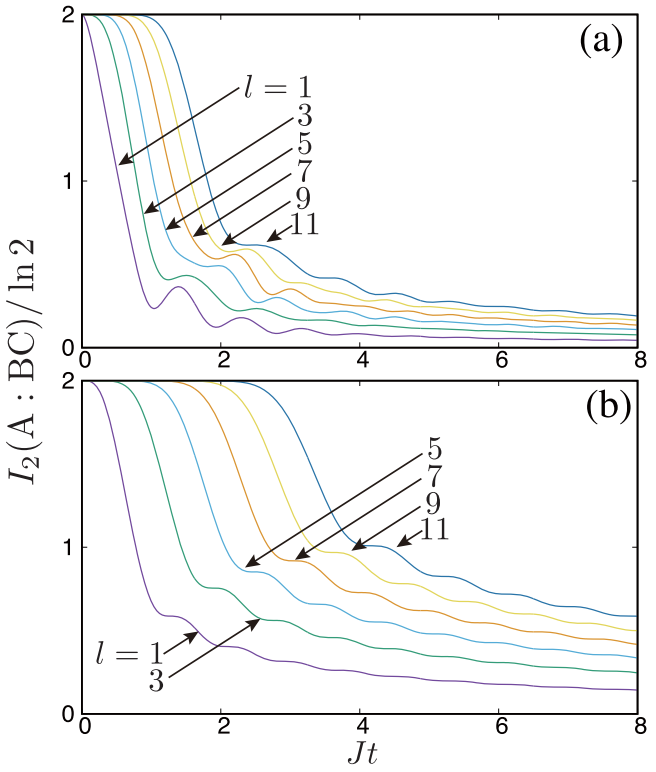

FIG. 11. Time dependence of BMI for (a) nonintegrable and (b) integrable *XXX* models. The system size is $L = 128$ and the initial state is all up.

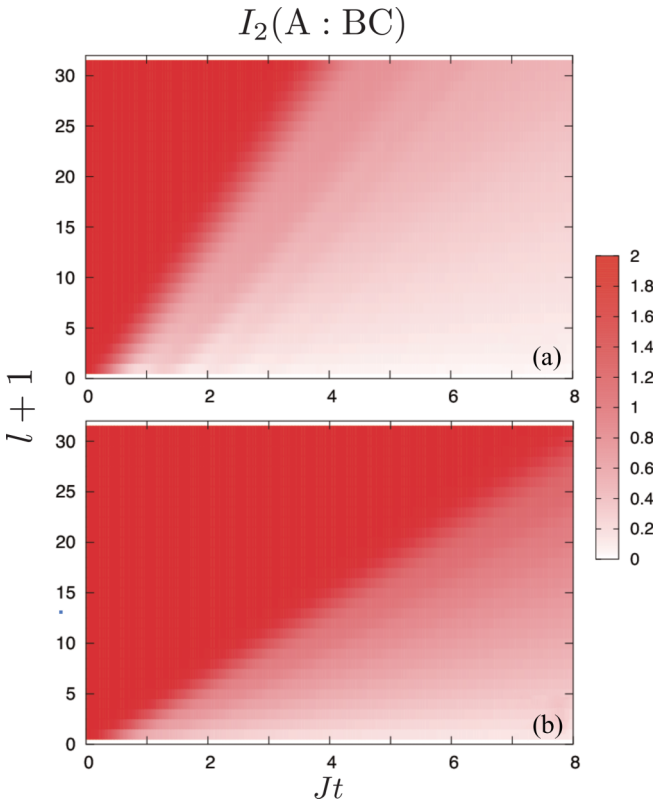

FIG. 12. BMI as a function of time t and subsystem size l for (a) nonintegrable and (b) integrable *XXX* models. The system size is $L = 128$ and the initial state is all up.

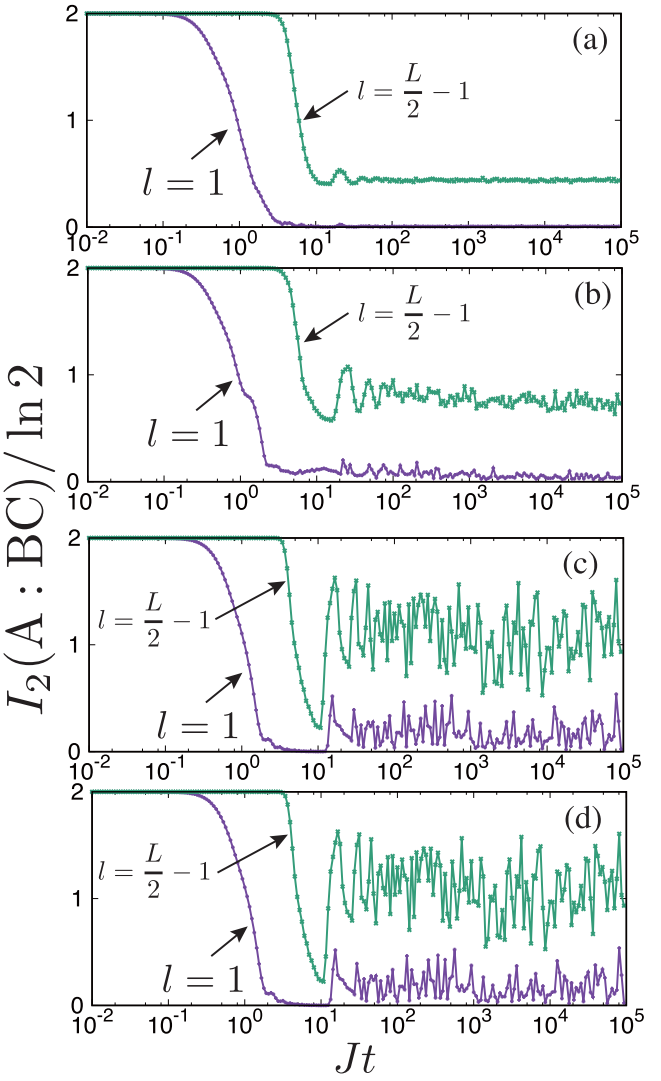

FIG. 13. Time dependence of BMI for the TFI model with $L = 14$. The integrability and the initial state are (a) nonintegrable, Néel, (b) nonintegrable, all up, (c) integrable, Néel, and (d) integrable, all up.

We first show numerical results on ballistic entanglement spreading for the integrable and nonintegrable *XXX* models. In particular, we consider the initial all-up state, where scrambling does not occur. In this case, we can numerically access a much larger size ($L = 128$) because the total magnetization is conserved in the *XXX* model. Figure 11 shows the time dependence of BMI for several l. Figure 12 shows BMI versus time and l, from which we again see the ballistic entanglement spreading.

Figures 13 and 14 show the time dependence of BMI and TMI for the TFI model (5), respectively. Figure 14 again shows that scrambling occurs independently of integrability or the initial state.

Figure 15 shows the time dependence of BMI and TMI for the disordered *XXX* model (6) with the initial all-up state. Figure 15(a) is similar to the time dependence of the clean *XXX* model. Figure 15(b) shows that entanglement spreading

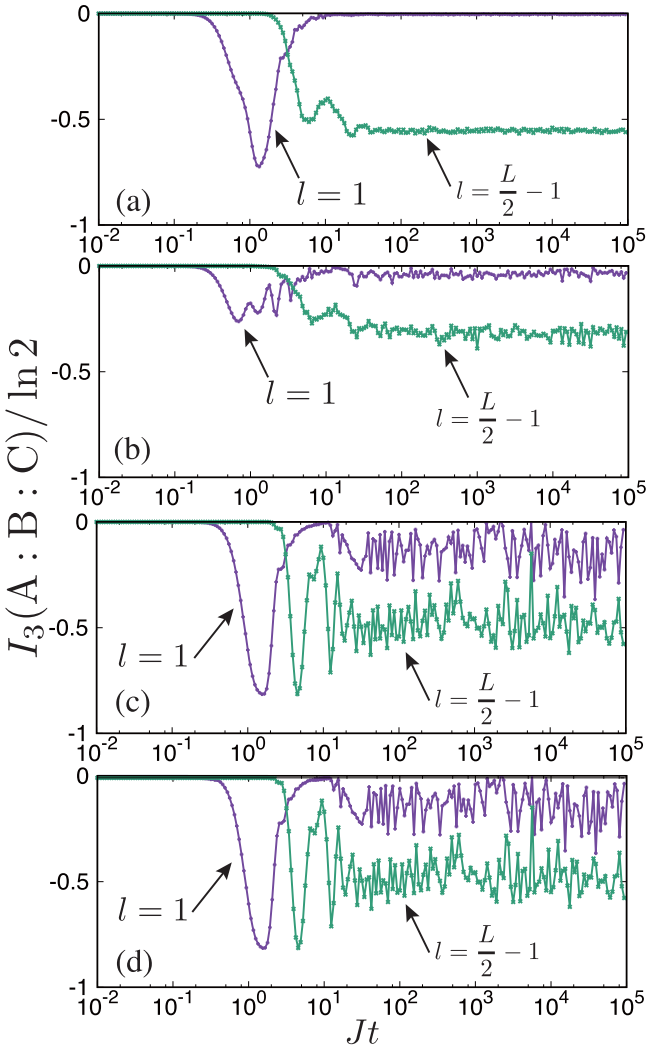

FIG. 14. Time dependence of TMI for the TFI model with $L = 14$. The integrability and the initial state are (a) nonintegrable, Néel, (b) nonintegrable, all up, (c) integrable, Néel, and (d) integrable, all up.

is quite slow, which is consistent with the phenomenology of the MBL phase [47].

Finally, Figs. 16(a) and 16(b) show the time dependence of BMI for the disordered SYK model with the initial Néel state and the initial all-up state. In the both cases, BMI decays irrespective of whether or not scrambling occurs.

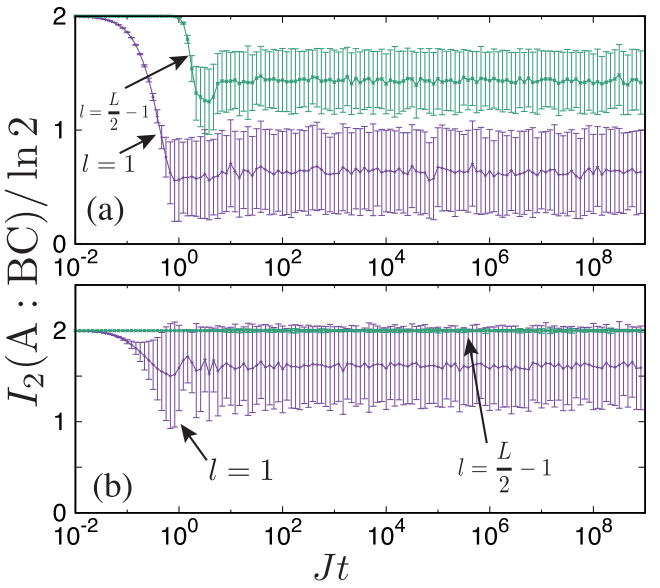

FIG. 15. Time dependence of BMI for the disordered *XXX* model with the initial all-up state with $L = 12$. The number of samples is 128. The phase is (a) ergodic ($h = J$) and (b) MBL ($h = 10J$).

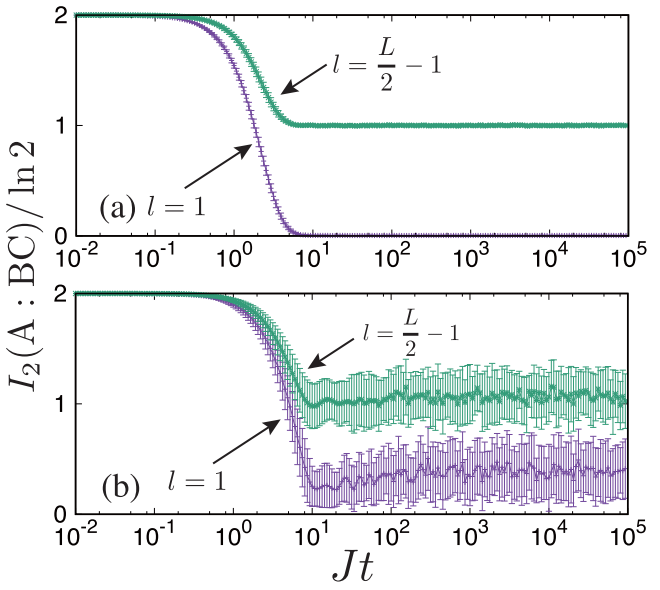

FIG. 16. Time dependence of BMI for the disordered SYK model. The ensemble average is taken over 16 samples. The initial state and the system size is (a) Néel, $L = 12$ and (b) all up, $L = 10$.

[1] G. Gallavotti, *Statistical Mechanics: A Short Treatise* (Springer, New York, 1999).

[2] H.-J. Stöckmann, *Quantum Chaos—An Introduction* (Cambridge University Press, Cambridge, 1999).

[3] Ph. Jacquod and D. L. Shepelyansky, Phys. Rev. Lett. **79**, 1837 (1997).

[4] L. F. Santos and M. Rigol, Phys. Rev. E **81**, 036206 (2010).

[5] T. Gorin, T. Prosen, T. H. Seligman, and M. Žnidarič, Phys. Rep. **435**, 33 (2006).

[6] A. Goussev, R. A. Jalabert, H. M. Pastawski, and D. Wisniacki, Scholarpedia **7**, 11687 (2012).

[7] M. Srednicki, Phys. Rev. E **50**, 888 (1994).

[8] M. Rigol, V. Dunjko, and M. Olshanii, Nature (London) **452**, 854 (2008).

[9] G. Biroli, C. Kollath, and A. M. Läuchli, Phys. Rev. Lett. **105**, 250401 (2010).

[10] L. D'Alessio, Y. Kafri, A. Polkovnikov, and M. Rigol, Adv. Phys. **65**, 239 (2016).

[11] E. Iyoda, K. Kaneko, and T. Sagawa, Phys. Rev. Lett. **119**, 100601 (2017).

[12] T. Kinoshita, T. Wenger, and D. S. Weiss, Nature (London) **440**, 900 (2006).

[13] M. Gring, M. Kuhnert, T. Langen, T. Kitagawa, B. Rauer, M. Schreitl, I. Mazets, D. A. Smith, E. Demler, and J. Schmiedmayer, Science **337**, 1318 (2012).

[14] S. Trotzky, Y.-A. Chen, A. Flesch, I. P. McCulloch, U. Schollwöck, J. Eisert, and I. Bloch, Nat. Phys. **8**, 325 (2012).

[15] G. Clos, D. Porras, U. Warring, and T. Schaetz, Phys. Rev. Lett. **117**, 170401 (2016).

[16] C. Neill, P. Roushan, M. Fang, Y. Chen, M. Kolodrubetz, Z. Chen, A. Megrant, R. Barends, B. Campbell, B. Chiaro, A. Dunsworth, E. Jeffrey, J. Kelly, J. Mutus, P. J. J. O'Malley, C. Quintana, D. Sank, A. Vainsencher, J. Wenner, T. C. White, A. Polkovnikov, and J. M. Martinis, Nat. Phys. **12**, 1037 (2016).

[17] P. Hayden and J. Preskill, J. High Energy Phys. 09 (2007) 120.

[18] Y. Sekino and L. Susskind, J. High Energy Phys. 10 (2008) 065.

[19] S. H. Shenker and D. Stanford, J. High Energy Phys. 03 (2014) 067.

[20] J. Maldacena, S. H. Shenker, and D. Stanford, J. High Energy Phys. 08 (2016) 106.

[21] P. Hosur, X.-L. Qi, D. A. Roberts, and B. Yoshida, J. High Energy Phys. 02 (2016) 004.

[22] N. J. Cerf and C. Adami, Physica D (Amsterdam) **120**, 62 (1998).

[23] A. Kitaev, A simple model of quantum holography (part 1), talk given at Entanglement in Strongly-Correlated Quantum Matter, April 7, 2015, http://online.kitp.ucsb.edu/online/entangled15/kitaev/; A. Kitaev, A simple model of quantum holography (part 2), talk given at Entanglement in Strongly-Correlated Quantum Matter, May 27, 2015, http://online.kitp.ucsb.edu/online/entangled15/kitaev2/.

[24] I. L. Aleiner, L. Faoro, and L. B. Ioffe, Ann. Phys. **375**, 378 (2016).

[25] F. M. Haehl, R. Loganayagam, P. Narayan, and M. Rangamani, arXiv:1701.02820.

[26] D. A. Roberts and B. Yoshida, J. High Energ. Phys. 04 (2017) 121.

[27] I. Kukuljan, S. Grozdanov, and T. Prosen, Phys. Rev. B **96**, 060301 (2017).

[28] E. B. Rozenbaum, S. Ganeshan, and V. Galitski, Phys. Rev. Lett. **118**, 086801 (2017).

[29] K. Hashimoto, K. Murata, and R. Yoshii, J. High Energ. Phys. 10 (2017) 138.

[30] P. Caputa, T. Numasawa, and A. Veliz-Osorio, Prog. Theor. Exp. Phys. **2016**, 113B06 (2016).

[31] P. Hayden, M. Headrick, and A. Maloney, Phys. Rev. D **87**, 046003 (2013).

[32] S. Ryu and T. Takayanagi, Phys. Rev. Lett. **96**, 181602 (2006).

[33] S. Sachdev and J. Ye, Phys. Rev. Lett. **70**, 3339 (1993).

[34] S. Sachdev, Phys. Rev. X **5**, 041025 (2015).

[35] B. Michel, J. Polchinski, V. Rosenhaus, and S. J. Suh, arXiv:1602.06422.

[36] J. Maldacena and D. Stanford, Phys. Rev. D **94**, 106002 (2016).

[37] W. Fu and S. Sachdev, Phys. Rev. B **94**, 035135 (2016).

[38] I. Danshita, M. Hanada, and M. Tezuka, Prog. Theor. Exp. Phys. **2017**, 083I01 (2017).

[39] J. S. Cotler *et al.*, J High Energ. Phys. 05 (2017) 118.

[40] S.-K. Jian and H. Yao, Phys. Rev. Lett. **119**, 206602 (2017).

[41] P. Calabrese and J. Cardy, J. Stat. Mech. (2005) P04010.

[42] A. M. Läuchli and C. Kollath, J. Stat. Mech. (2008) P05018.

[43] H. Kim and D. A. Huse, Phys. Rev. Lett. **111**, 127205 (2013).

[44] A. Bohrdt, C. B. Mendl, M. Endres, and M. Knap, New J. Phys. **19**, 063001 (2017).

[45] A. Pal and D. A. Huse, Phys. Rev. B **82**, 174411 (2010).

[46] J. H. Bardarson, F. Pollmann, and J. E. Moore, Phys. Rev. Lett. **109**, 017202 (2012).

[47] M. Serbyn, Z. Papić, and D. A. Abanin, Phys. Rev. Lett. **111**, 127201 (2013).

[48] D. J. Luitz, N. Laflorencie, and F. Alet, Phys. Rev. B **91**, 081103 (2015).

[49] Y. Huang, Y.-L. Zhang, and X. Chen, Ann. Phys. **529**, 1600318 (2016).

[50] Y. Chen, arXiv:1608.02765.

[51] R. Fan, P. Zhang, H. Shen, and H. Zhai, Sci. Bull. **62**, 707 (2017).

[52] B. Swingle and D. Chowdhury, Phys. Rev. B **95**, 060201 (2017).

[53] A. Kitaev and J. Preskill, Phys. Rev. Lett. **96**, 110404 (2006).

[54] P. Reimann, Phys. Rev. Lett. **101**, 190403 (2008).

[55] M. L. Mehta, *Random Matrices* (Academic, San Diego, 2004).

[56] L. Samaj and Z. Bajnok, *Introduction to the Statistical Physics of Integrable Many-body Systems* (Cambridge University Press, Cambridge, 2013).

[57] E. Iyoda, H. Katsura, and T. Sagawa (unpublished).

[58] D. I. Pikulin and M. Franz, Phys. Rev. X **7**, 031006 (2017).

[59] M. Gärttner, J. G. Bohnet, A. Safavi-Naini, M. L. Wall, J. J. Bollinger, and A. M. Rey, Nat. Phys. **13**, 781 (2017).